JPL Document D-77698

Exoplanet Exploration Program Technology Plan

Appendix: 2012

P. R. Lawson

National Aeronautics and
Space Administration

Jet Propulsion Laboratory
California Institute of Technology
Pasadena, California

11 February 2013

This reseach was carried out at the Jet Propulsion Laboratory, California Institute of Technology, under a contract with the National Aeronautics and Space Administration.

Approvals

Released by

2/11/2013

Peter Lawson, Exoplanet Exploration Program Chief Technologist, JPL

Approved by

2/11/2013

Gary Blackwood, Exoplanet Exploration Program Manager, JPL

2/11/2013

Douglas Hudgins, Exoplanet Exploration Program Scientist, NASA HQ

2/11/2013

Anthony Carro, Exoplanet Exploration Program Executive, NASA HQ

Concurrences

2/11/13

Marie Levine, Exoplanet Exploration Program Technology Manager, JPL

4 Feb. 2013.

Wesley Traub, Exoplanet Exploration Program Chief Scientist, JPL

Contents

Appendix A
Exoplanet Technology Plan Milestones

A.1 Introduction

The purpose of this appendix is to guide near-term (1–5 year) technology development for future space observatories related to NASA's Exoplanet Exploration Program (ExEP). The long-term goal of this technology development is to enable a mission capable of detecting and characterizing the spectra of Earth-like exoplanets and measuring the atmospheric signatures of life. Through this work it should also be possible in the near term to enable other missions whose science is compelling and essential to understanding the birth and evolution of planetary systems and the conditions that lead to life in the Universe.

The subjects covered here are only those most directly relevant to recommendations in the 2010 Decadal Survey of Astronomy and Astrophysics (Astro2010) [1], with regard to a *New Worlds Technology Development Program* and a future *New Worlds Mission*. The greatest emphasis is therefore placed on the detection of Earth-like planets around Sun-like stars and the development of starlight-suppression technology.

To date, the greatest advances in exoplanet science have been through what could be called "combined-light" techniques, where no attempt is made to suppress starlight or to spatially resolve the star-planet system. These approaches all infer the presence of planets by measuring small changes in the intensity, spectrum, or relative angular position of stars, and are limited in sensitivity either by aperture size, in the case of radial-velocity measurements, or by atmospheric scintillation and phase noise, in the case of transit, microlensing, and astrometry measurements. The most prolific exoplanet detection technique to date has been the radial velocity technique, which has yielded over 60% of the more than 800 known exoplanets. Transit observations have detected about 30% of all confirmed planets, and NASA's *Kepler* mission, has yielded an additional 2320 exoplanet candidates as of November 2012, a large fraction of which may ultimately be confirmed. Ground-based microlensing measurements have added to the total about a dozen Super-Earth planets in Earth- and Mars-like orbits, plus a handful of free-floating planets. Finally, astrometric measurements have yielded one planet twice the mass of Jupiter. For all these techniques except the radial velocity technique, there are great advantages of going to space, and few if any technical challenges. Not surprisingly, NASA and ESA both are studying transit and microlensing missions as components of their mission portfolios in the coming decade.

However, as exciting and scientifically important as the ongoing combined-light studies are to our understanding of exoplanets and exoplanetary systems, the long-term goal of NASA's Exoplanet Exploration Program cannot be achieved through such indirect measurement.

The ultimate goal of the Program is a New Worlds mission, such as that envisaged by Astro2010: a mission capable of directly imaging terrestrial planets in the habitable zones of stars in the Solar neighborhood, and measuring their spectra to search for the telltale signs of life. Such a mission will require some form of starlight suppression, and new technology developments will be needed to achieve the extreme degree of contrast that will be required. The necessary technology developments and ongoing activities are summarized in this appendix. An excellent overview of the challenges of direct imaging can be found in the volume *Exoplanets*, edited by S. Seager [2]. The interested reader will find additional details concerning exoplanet technology in the SPIE Conference Series on *Techniques and Instrumentation for the Detection of Exoplanets*, the most recent being Proc. SPIE vol. 8151. Further papers of interest can be found in Proc. SPIE vol. 8442, in particular the invited review by D. Mawet [3].

The goals of the Exoplanet Exploration Program for technology development are described in Section A.2. The driving science requirements and the technology priorities are described in Section A.3. Details of future technology milestones for coronagraphs, starshades, and interferometers are then given in sections A.4, A.5, and A.6 respectively.

A.2 Program Goals

The 2010 Decadal Survey in Astronomy and Astrophysics (NRC 2010) recommended the creation of a *New Worlds Technology Development Program* to advance the technological readiness of the three primary starlight suppression architectures: coronagraphs, starshades, and interferometers. The Survey further recommended—if the scientific groundwork and design requirements were sufficiently clear—that an architecture downselect should be made at the mid-decade, and a significantly increased technology investment over the latter half of the decade should be focused to prepare a mission concept based on this architecture for consideration by the 2020 Survey.

NASA's Exoplanet Exploration Program supports activities that will contribute to the selection and advancement of one or more exoplanet mission concepts to a high Technology Readiness Level (TRL). The Program funds and facilitates experiments and analyses selected by NASA HQ through yearly solicitations issued through the NASA omnibus Research Opportunities in Space and Earth Sciences (ROSES). The Program also provides support in the form of infrastructure, expertise, and test facilities that have been developed in prior years.

NASA currently funds technology development through the Astrophysics Research and Analysis (APRA) solicitation and the Technology Development for Exoplanet Missions (TDEM) component of the Strategic Astrophysics Technology (SAT) solicitation. APRA covers low-TRL technology research while SAT-TDEM covers maturation of mid-range TRL technologies. This two-stage approach supports the advancement of technology envisaged by Astro2010. TDEM tasks funded for the 2009 and 2010 solicitations are listed in Tables A.1 and A.2.

Table A.1: Starlight Suppression Technology research funded through the Technology Development for Exoplanet Missions component of NASA's solicition on Strategic Astrophysics Technology. Awards for calls from 2009 and 2010 are listed. Each award nominally provides two years of funding. The 2009 awards were funded in 2010 and so will continue through 2012. The 2010 awards were funded in 2012 and so should continue through 2014. These efforts are described in further detail in Section A.4 and A.5.

Year	PI	Institution	Proposal Title
LYOT CORONAGRAPH MASK TECHNOLOGY			
2009	John Trauger	JPL/Caltech	Advanced Hybrid Lyot Coronagraph Technology for Exoplanet Missions
2010	Eugene Serabyn	JPL/Caltech	Demonstrations of Deep Starlight Rejection with a Vortex Coronagraph
PHASE INDUCED AMPLITUDE APODIZATION			
2009	Olivier Guyon	Univ. of Arizona	Phase-Induced Amplitude Apodization Coronagraphy Development and Laboratory Validation
2010	Olivier Guyon	Univ. of Arizona	Advances in Pupil Remapping (PIAA) coronagraphy: improving Bandwidth, Throughput and Inner Working Angle
VISIBLE NULLING CORONAGRAPH TECHNOLOGY			
2009	Mark Clampin	NASA/GSFC	Visible Nulling Coronagraph Technology Maturation: High Contrast Imaging and Characterization of Exoplanets
2010	Richard Lyon	NASA/GSFC	Compact Achromatic Visible Nulling Coronagraph Technology Maturation
2010	Jagmit Sandhu	JPL/Caltech	Visible Nulling Coronagraph (VNC) Technology Demonstration Program
STARSHADE TECHNOLOGY			
2009	N. Jeremy Kasdin	Princeton University	Starshades for Exoplanet Imaging and Characterization: Key Technology Development
2010	N. Jeremy Kasdin	Princeton University	Verifying Deployment Tolerances of an External Occulter for Starlight Suppression

The goal of exoplanet technology development is to enable future missions by demonstrating selected key technologies. This effort must include the establishment of performance error budgets tied to flight requirements and experimental demonstrations that the error budgets, or key components of the error budgets, can be met. Furthermore, models must be validated that demonstrate that the physics of the limiting error sources in those experiments are understood well enough to reliably predict the performance of the flight mission.

Table A.2: Supporting Technologies research funded through the Technology Development for Exoplanet Missions component of NASA's solicition on Strategic Astrophysics Technology. Awards for calls from 2009 and 2010 are listed. These efforts are described in further detail in Section A.4 and A.7.

Year	PI	Institution	Proposal Title
WAVEFRONT SENSING & CONTROL			
2009	Martin Noecker	Ball Aerospace	Advanced Speckle Sensing for Internal Coronagraphs and Methods of Isolating Exoplanets from Speckles
2010	N. Jeremy Kasdin	Princeton University	Integrated Coronagraph Design and Wavefront Control using Two Deformable Mirrors
2010	Paul Bierden	Boston Micromachines Corporation	MEMS Deformable Mirror Technology Development for Space-Based Exoplanet Detection
2010	Michael Helmbrecht	Iris AO	Environmental Testing of MEMS Deformable Mirrors for Exoplanet Detection
MODELING AND MODEL VALIDATION			
2009	John Krist	JPL/Caltech	Assessing the Performance Limits of Internal Coronagraphs Through End-to-End Modeling
2010	Stuart Shaklan	JPL/Caltech	Coronagraph Starlight Suppression Model Validation: Coronagraph Milestone #3A
DETECTOR TECHNOLOGY*			
2009	Donald Figer	Rochester Inst. Tech.	A Photon-Counting Detector for Exoplanet Missions

* Topic area excluded from the TDEM element of SAT in subsequent ROSES calls.

A.3 Science & Technology Objectives

Science Objectives

The science objectives that motivate technology development within the Exoplanet Exploration Program are focused on the discovery and characterization of *Earth-like* exoplanets. The principal goals are to directly detect and characterize Earth-like planets around nearby stars and to search for signs of habitability and life. For observations at optical and near-infrared wavelengths, the science objectives apply as formulated in 2006 by the Terrestrial Planet Finder Coronagraph (TPF-C) Science and Technology Definition Team (STDT) [4]. The first four objectives, describing terrestrial planet science, are as follows:

1. Directly detect terrestrial planets within the habitable zones around nearby stars, or alternatively, show that they are not present.
2. Measure orbital parameters and brightnesses for any terrestrial planets that are discovered.

3. Distinguish among planets, and between planets and other objects, through measurements of planet color.
4. Characterize at least some terrestrial planets spectroscopically, searching for absorption caused by O_2, O_3, H_2O, and possibly CO_2 and CH_4. It is highly desirable to measure Rayleigh scattering and photosynthetic pigments; such information may provide evidence of habitability and even of life itself.

Closely similar science objectives were also established for the Terrestrial Planet Finder Interferometer (TPF-I) for observations at mid-infrared wavelengths [5].

Up until now, the TPF science objectives have not been reformulated for the Program; they continue to be well aligned with the priorities articulated in the 2010 Astrophysics Decadal Survey. They will nonetheless be reevaluated and revised as appropriate by the Exoplanet Exploration Program Analysis Group (ExoPAG). Until such time, the TPF science objectives [4][5] continue to be adopted.

These science objectives have been used to derive the required starlight rejection, angular resolution, inner working angle, sensitivity, bandwidth, and corresponding error budgets for the TPF missions. They can be equally applied to deriving performance requirements for a future *New Worlds Mission*.

Performance Requirements

The key instrument performance requirement that drives the technology effort is the ability to suppress starlight to a level where the detection of Earth-like planets becomes possible. Fig. A.1 shows the performance limits of current coronagraphs, and the expected performance of future ground and space-based systems. The curves that are shown represent 5-σ detection limits for 1-hour observations. The most ambitious ground-based coronagraphs are represented by proposed instruments on the Thirty Meter Telescope (TMT PFI) and the European Extremely Large Telescope (E-ELT EPICS), whose predicted performance corresponds to contrasts of 10^{-8} or slightly better. The fundamental limitation of a ground-based coronagraph is determined by the residual atmospheric wavefront error left uncorrected by an adaptive optics system. The RMS wavefront error corresponding to a given contrast is shown on the left-hand side of Fig. A.1 and to achieve higher contrast, the adaptive optics must operate correspondingly faster, requiring even brighter target stars. There are no stars bright enough in the sky that allow contrasts approaching 10^{-9} to be achieved from the ground using adaptive optics. To detect Earth-like planets, a space telescope is required.

At visible wavelengths, Earth-like planets shine in reflected starlight and change in brightness according to the phase of their orbits. The light curves for Solar-system planets is illustrated by the light gray curves toward the bottom and left in Fig. A.1. To detect a sample of Earth-like planets the corresponding requirement is for an observatory to be capable of detecting exoplanets up to 26 magnitudes fainter than their host stars, implying a performance level enabling contrasts of better than 10^{-10} at visible wavelengths. At mid-infrared wavelengths, planets shine in their own thermal emission, and have a wavelength-dependent planet/star contrast of 10^{-6}–10^{-7}. A mid-infrared observatory must be capable of suppressing starlight and background sources to a contrast level of 10^{-8}.

An angular resolution and inner working angle are required that allow a sufficiently large sample of candidate stars to be imaged such that orbiting planets can be distinguished as separate from the star itself and from each other. Within the central field of view, inside the inner working angle, no planets are detectable because their light is suppressed along with the starlight. For coronagraphs, inner working angles of 2–4 λ/D seem achievable. For starshades, the inner working angle is determined by the starshade diameter and distance from the telescope. A smaller inner working angle is greatly advantageous, but imposes severe stability requirements on the telescope system for coronagraphs, or much larger separations from the telescope in the case of starshades. There are therefore several important design trades to be made in the architectures of exoplanet missions. The inner working angle should be ~65 mas or smaller to detect a reasonable sample of planets, implying the need at optical wavelengths for primary mirrors of 4-m or larger if Earth-like planets are to be detectable.

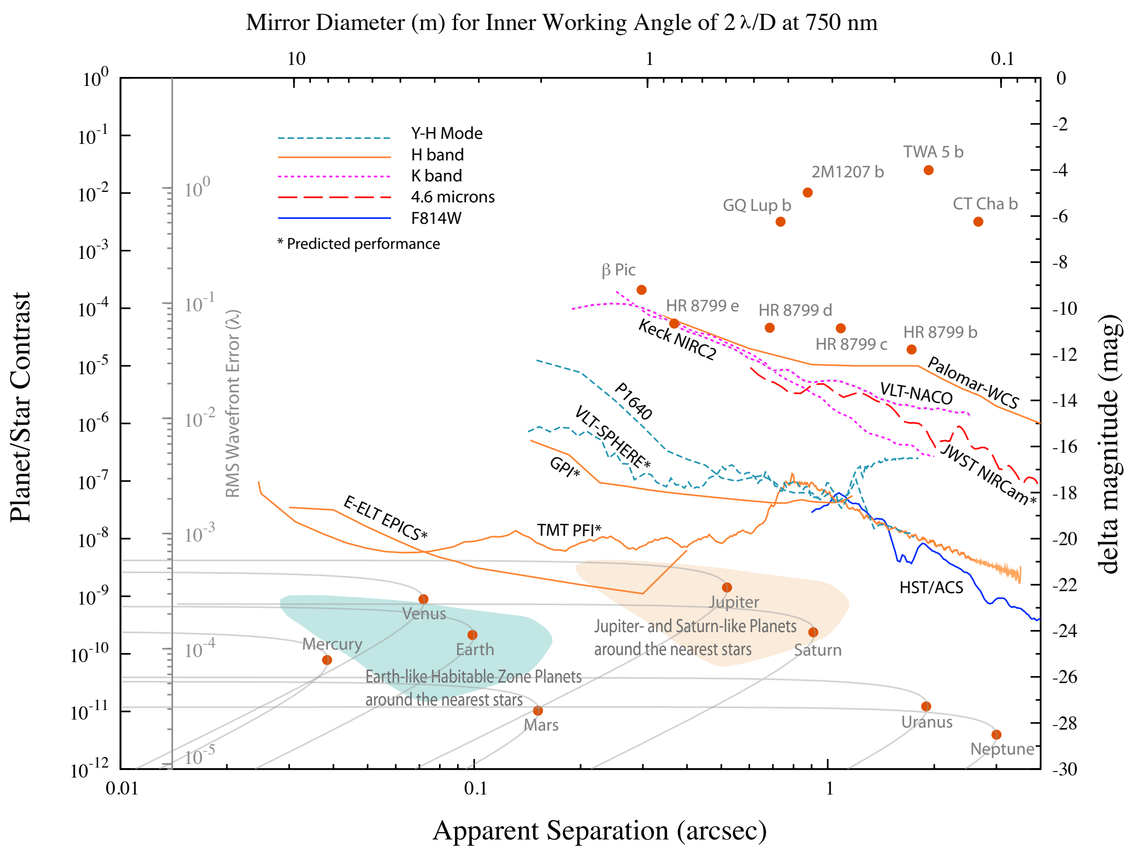

Figure A.1. Current and planned future capabilities in ground and space-based coronagraphy.

The required mirror quality of large optics need be no better than that of the primary mirror of the Hubble Space Telescope. For coronagraphs, deformable mirrors are used for fine wavefront sensing and control, providing wavefront quality at the sub-nanometer level. Large-mirror technology is therefore not seen to be an area of concern in the development of exoplanet missions.

For coronagraphs, the required instrument pointing stability is dependent on the instrument design and for the most aggressive coronagraphs is at the sub-milliarcsecond level. This can be accomplished using wavefront sensing and control prior to the mask and through the use of a low-order wavefront sensor to actively correct the fine pointing and the lower order aberrations. For starshades the equivalent concern is off-axis starshade/telescope tracking, which must be controlled at about the 0.75-m level.

The starlight suppression requirements, described above, hold true irrespective of the mission architecture. The technology milestones described in the TPF technology plans for detecting and characterizing Earths [6][7] remain valid, because the contrast goals are independent of the telescope size. In those plans, demonstrated laboratory performance within an order of magnitude of the flight requirement—10^{-9} at visible wavelengths and 10^{-5}–10^{-6} at mid-infrared wavelengths—was deemed sufficient to proceed to Phase A. These performance requirements have therefore also been adopted.

Technology Priorities

The recommendation by the Decadal Survey was to continue to pursue the development of coronagraph, external occulter, and interferometer technologies to allow an architecture downselect by the late-Decade. Nevertheless, for both cost and technical readiness reasons, infrared interferometry is currently of lower priority as the basis for a *New Worlds Mission* than either of the coronagraph or starshade architectures.

The highest priority technology demonstrations for all architectures are the following:

1. Experimental demonstrations that the necessary starlight suppression is achievable;
2. System-level demonstrations that the required starlight suppression can be maintained with adequately stability within the observatory, when subjected to realistic on-orbit disturbances; and
3. The validation of models and error budgets that demonstrates the physics of starlight suppression including the dominant sources of instrument noise are understood within the accuracy required for on-orbit performance prediction.

Demonstrations that emphasize approaches that provide high-sensitivity and a small inner working angle are particularly valued as they may greatly increase the science return from a mission.

The above demonstrations by themselves take precedence over any other related technologies, including detector technology, mirror technology (with the exception of adaptive systems), telescope assembly technology, sunshields and isothermal control, propulsion systems, vibration isolation systems, spacecraft pointing control, or formation flying technology. The SAT-TDEM solicitation may list specific technologies that are excluded from consideration in a given year, and the reader is encouraged to carefully review each solicitation for details.

Technology Milestones

After each cycle of awards, the Program works individually with each SAT-TDEM PI to establish one or more formal milestones for their mid-level TRL research efforts. The PIs document their intended objective in a whitepaper that stipulates a performance threshold representing a meaningful advance in technology. The research goals must be traceable to a mission error budget, and model predictions must be based on experimental results. The whitepaper describes the experiment or modeling effort that will be undertaken, specifes the methodology for computing a milestone metric, and establishes success criteria against which the milestones will be evaluated. Amongst these success criteria is invariably a requirement that the technology performance threshold be achieved repeatedly in order to demonstrate the robustness of the technology. The whitepapers are reviewed by the ExEP Technology Assessment Committee and formally approved by the Program. The completion of a milestone is later to be documented in a report by the PI, which is then reviewed and similarly approved. The Milestone Whitepapers that have been completed to date can be found at http://exep.jpl.nasa.gov/technology/.

The following sections outline the technology milestones for coronagraphs, starshades, and interferometers.

A.4 Coronagraph Milestones

There are several approaches to the design of coronagraph instruments. Such instruments may include implementations of intensity masks [8], phase masks [9], phase-induced amplitude apodization [10], shaped pupils [11], visible nulling coronagraphs [12], or hybrid designs [13].

The state of the art demonstrated in the lab is summarized in Fig. A.2. Most notable amongst these results is a contrast of 2×10^{-10} with a 2% bandwidth and 2×10^{-9} with a 20% bandwidth at 3–15λ/D achieved through the use of 4th order band-limited Lyot hybrid masks [14]. Models exist that match these results, although they have not yet been formally validated. Other results plotted in Fig. A.2 are described later in the text.

The milestones below are paraphrased from the TPF-C Technology Plan [7] and Milestone documents [15][17][18]. The first milestone demonstrates the feasibility of starlight suppression. The second demonstrates that it is applicable over a representative science band. The third demonstrates that the physics models are well understood and the known sources of noise are controlled, thus validating the error budget for the most problematic sources of system degradation. The fourth demonstrates through observatory simulation, combined with experimental results, that the mission could achieve its stated science goals. These milestones are progressive and sufficiently generalized to be applicable to any optical coronagraph mission concept. These are the most significant high-level milestones to be accomplished in pre-Phase A. SAT-TDEM research may support these milestones themselves, or partial progress toward these goals.

As listed below, Milestones 1 and 2 have been completed using a band-limited mask, as described in section A.4.1 and denoted by the filled red squares in Fig. A.2. These milestone results have since been surpassed by subsequent band-limited metal and hybrid masks but those results were not formally reviewed. To date no other approach has performed as well. The motivation for continued support of competing methods is to raise the technology level of new instrument designs that may yet provide improved science throughput. The milestones are as follows:

Milestone 1. Narrow-band Starlight Suppression. Demonstrate monochromatically the technology for Earth-like planet detection by optical starlight suppression to a level within an order of magnitude of the required flight performance. Using monochromatic light at an optical wavelength in the intended science band, a contrast of less than 1×10^{-9} must be achieved in a target dark hole whose inner working angle is representative of the flight mission. The demonstration must be repeated on three separate occasions.

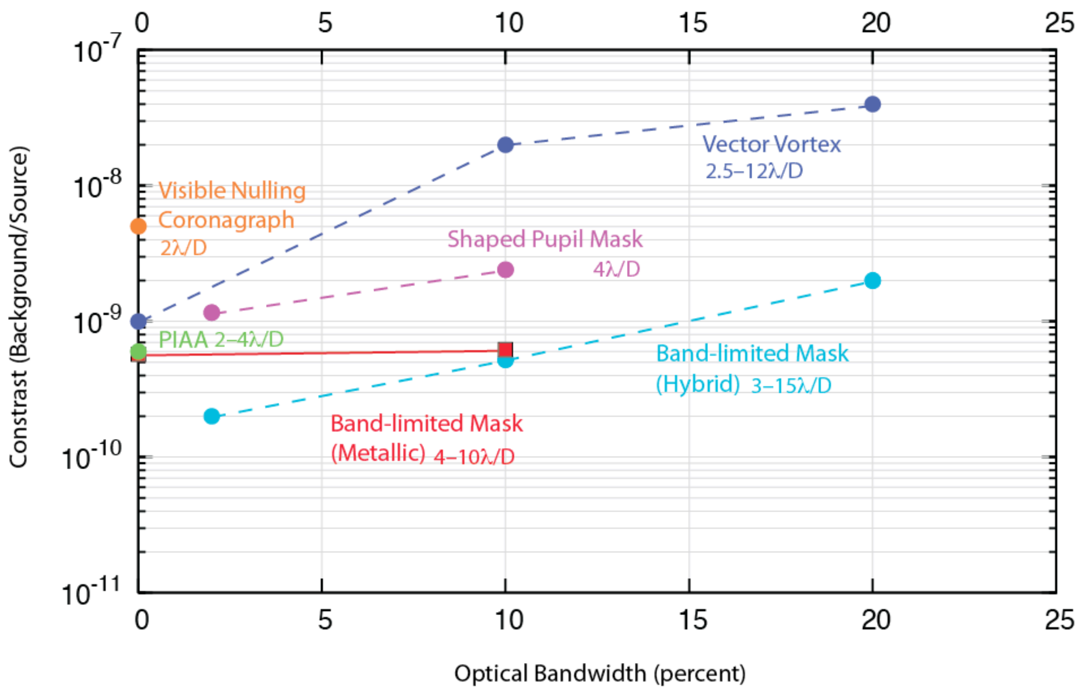

Fig. A.2: Demonstrated coronagraph contrast as a function of bandwidth. This plot summarizes results described in the text. Results reported by PIs or found in the published literature are denoted by the filled circles. Milestone results are denoted by the filled squares. The mean contrast is plotted for results that are averaged over a dark hole, ie. averaged over an area of 4–10 λ/D in the case of the metallic band-limited mask. The Earth/Sun contrast at visible wavelengths would be approximately 10^{-10}.

Milestone 2. Broad-band Starlight Suppression. Demonstrate with broadband light the technology for Earth-like planet detection by optical starlight suppression to a level within an order of magnitude of the required flight performance. Using broadband light with a fractional bandwidth $\Delta\lambda/\lambda \geq 10\%$ centered at an optical wavelength in the intended science band, a contrast of less than 1×10^{-9} must be achieved in a target dark hole whose inner working angle is representative of the flight mission. The demonstration must be repeated on three separate occasions.

Milestone 3A. Model Validation of Starlight Suppression. Demonstrate that starlight suppression performance predictions from high-fidelity optical models of experiments, using measured data on specific testbed components, are consistent with actual measured results on the testbed. The correlation of model predictions with experimental testbed results thus validates models at a baseline contrast ratio of better than 1×10^{-9} (goal 1×10^{-10}). The measurement to be evaluated is the comparison between the contrast predicted by the model and the contrast achieved in the experiment. Broadband light must be used with a fractional bandwidth $\Delta\lambda/\lambda \geq 10\%$ centered at an optical wavelength in the intended science band. The contrast metrics must be demonstrated in a target dark hole representative of the flight mission.

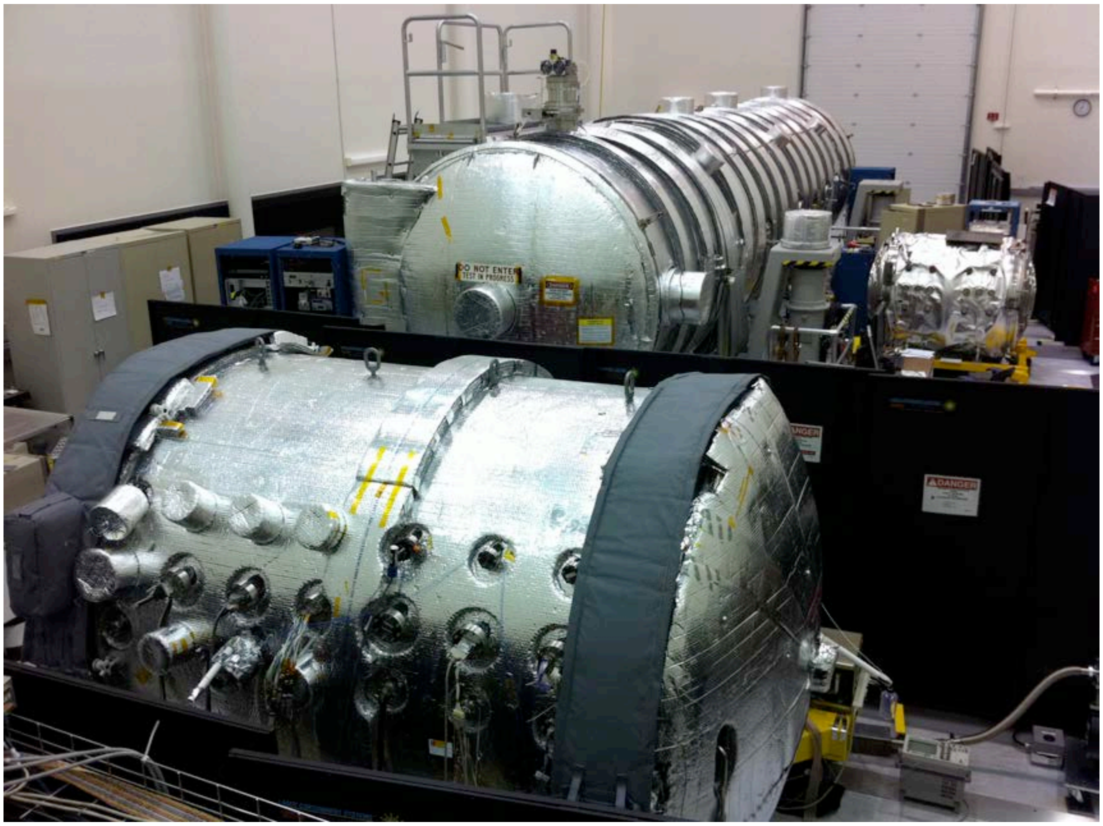

Fig. A.3. The Exoplanet Exploration Program facilities at the Jet Propulsion Laboratory. The High Contrast Imaging Testbed (HCIT-1) is in the foreground. It currently houses experiments that use hybrid Lyot masks and vector vortex masks. The HCIT-2 facility is the large tank in the top center. It currently supports experiments in Phase-Induced Amplitude Apodization (PIAA). The APEP facility, which houses a visible nulling testbed is the smaller tank seen in the upper right of the photo. These facilities are located in the highbay of Building 318.

Milestone 3B. Demonstrate, using the modeling approach validated against experimental results (above) combined with appropriate telescope models and the current mission error budget, that a coronagraph could achieve a baseline contrast of 1×10^{-10} over the required optical bandwidth necessary for detecting Earth-like planets, characterizing their properties and assessing habitability.

Progress toward achieving the above high-level milestones could be marked by milestones in other key technologies. Related activities could include, but are not limited to, (a) demonstrations of wavefront control through the simultaneous use of two deformable mirrors, (b) the development of special-purpose optics such as image-plane masks or apodizing optics, (c) maturation of deformable mirror technologies, (d) advances in modeling high-contrast imaging optical systems, (e) the ability to suppress starlight in the presence of flight-like and time-varying low-order wavefront errors, and (f) demonstrations of astrometry techniques that are compatible with starlight suppression systems.

Future milestones would include those related to structural, thermal, and spacecraft technology demonstrated at the component, subsystem, and system level. A key milestone in this regard would be a precision structure stability demonstration.

Space-based coronagraphs are typically designed to work with off-axis telescopes to provide an unobscured entry pupil—without the unwanted diffraction from a secondary mirror and its support structure. Several approaches have been proposed that nonetheless promise to perform well, even in the presence of partially obscured or segmented primary mirrors [19][20][21][22], thus providing perhaps new opportunities to integrate coronagraph instruments with space telescopes that were designed for other applications.

The Exoplanet Exploration Program maintains facilities at the Jet Propulsion Laboratory to enable vacuum experiments in high-contrast imaging. The facilities are shown in the photograph of Fig. A.3. Up until 2011, all coronagraph experiments at JPL—with the exception of visible nulling—were conducted in the original High Contrast Imaging Testbed (HCIT), seen in the foreground of Fig. A.3. Two separate optical tables were used: one devoted to Lyot-type experiments, and one to Phase Induced Amplitude Apodization (PIAA) experiments. These were exchanged in the HCIT depending on the need. In 2011, JPL's Micro-Arcsecond Metrology vacuum chamber was converted into a second High Contrast Imaging Testbed (HCIT-2) to support PIAA coronagraphy. The original HCIT is now dedicated solely to demonstrating coronagraphs compatible with Lyot optical configurations. Additionally, in 2012 the smaller APEP vaccum chamber was commissioned to support Visible Nulling Coronagraphy. In Fig. A.3 the HCIT-2 is in the top-middle of the photo and the APEP testbed on the top-right.

A.4.1 Progress and Plans

Lyot Coronagraph Mask Technology

Band-limited Lyot Masks

Milestones 1 and 2 were completed by the TPF-C Pre-Project for an instrument design employing a linear 4th-order band-limited mask [15][17]. This mask used an intensity-only design.

No further development of masks of this exact same design is anticipated because its performance degrades at larger bandwidths and smaller inner working angles. Subsequent work on masks of this type, described below, has focused on an improved *hybrid* design that includes a dielectric layer to compensate for small phase errors induced by the metallic intensity mask. Nonetheless, band-limited Lyot masks that were developed by the TPF-C Pre-Project will be used in experiments for coronagraph model validation.

Band-limited Hybrid Lyot Masks

The state-of-the-art in coronagraphic starlight suppression is represented by results obtained with hybrid Lyot masks in the HCIT, which have surpassed the performance demonstrated with masks using the intensity-only designs. In 2011 a contrast was demonstrated of 2.0×10^{-10} with a bandwidth of 2%, 5.2×10^{-10} with a bandwidth of 10%, and 2.0×10^{-9} with a bandwidth of 20%, all using a dark hole extending over 3–15λ/D. The primary goal of work had been to obtain contrasts better than 1.0×10^{-9} with bandwidths of 20%. The limiting factor was identified as an error in the mask fabrication. Future work may include improvements in mask fabrication techniques, operation in two shorter wavelength bands, and the implementation of circular rather than linear hybrid masks.

This work was the subject of a 2009 TDEM award to John Trauger (JPL/Caltech) and collaborators. A technology milestone whitepaper was approved by the Program to formalize the goals of this research [23]. A final report is pending.

Vector Vortex Masks

Experiments with vector vortex masks in the HCIT in 2012 achieved a contrast of $\sim 1.0 \times 10^{-9}$ in monochromatic light. Prior results in 2011 reported 2×10^{-8} with a 10% bandwidth, and 4×10^{-8} with a 20% bandwidth at 2.5–12λ/D [30]. Identical masks have been used to detect exoplanets with the Palomar 5-m telescope [31] and may be used with on-axis telescopes [32]. A technology milestone whitepaper was approved by the Program to formalize the goals of monochromatic contrast demonstrations [33]. This phase of effort is nearing completion.

Broadband demonstrations with vector vortex masks are being led by Eugene Serabyn (JPL/Caltech), funded through a 2010 SAT-TDEM award.

Shaped Pupil Masks

Vacuum experiments with shaped-pupil masks in the HCIT have yielded contrasts of 1.16×10^{-9} with a 2% bandwidth and 2.4×10^{-9} with a 10% bandwidth, both at inner working angles of 4λ/D [39]. This work was led by Ruslan Belikov (now NASA ARC) and Jeremy Kasdin (Princeton University), but was not the subject of a formal Program milestone.

Ongoing work is being led by Jeremy Kasdin (Princeton Univ.) and includes the implementation of a hybrid design that combines shaped pupils with a pair of deformable mirrors with the goal of enabling a higher throughput at a smaller inner working angle [40] [41]. This approach is also being applied to cases where the telescope aperture is segmented or partially obscured. No formal milestones goals have been established for this effort, as the support for this work has been independent of SAT-TDEM.

Phase-Induced Amplitude Apodization

Phase-Induced Amplitude Apodization uses pairs of aspheric mirrors to reshape the intensity distribution passing through an aperture, providing a Gaussian-like distribution and eliminating diffraction sidelobes. Supporting work toward this goal is being conducted at the NASA Ames Coronagraph Experiment (ACE) and at the HCIT-2 at JPL/Caltech. The research at ACE is conducted in air using a thermally stabilized enclosure, permitting initial validation (TRL 1–4) of PIAA and related technologies that can then be validated at higher TRL levels (TRL 4+) using the vacuum facility of the HCIT.

Experiments at ACE in 2011 achieved a contrast of 1.9×10^{-8} using a paired-mirror system, in monochromatic light at an inner working angle of 2λ/D [25]. In 2012, a new low-order wavefront sensor was implemented within the HCIT-2 to improve the pointing required at small inner working angles, and subsequent paired-mirror experiments achieved a contrast of 6.0×10^{-10} in monochromatic light at 2λ/D; a formal report of this work is being prepared.

Work with the HCIT-2 at JPL/Caltech is being conducted by Olivier Guyon (Univ. Arizona) and collaborators, currently supported by a 2009 TDEM award. Two technology milestone whitepapers were approved by the Program to formalize the goals of this research: one for demonstrations of monochromatic contrast [27] and one for demonstrations of sub-milliarcsecond pointing stability [28]. The pointing demonstration was successfully completed, and the monochromatic demonstrations are nearing completion. Broadband contrast demonstrations will be the subject of continuing work by the same investigators, supported through a 2010 SAT-TDEM award.

Visible Nulling Coronagraph Technology

A visible nulling coronagraph uses an interferometer back-end to reject starlight via interferometric nulling with a sheared pupil. This approach uses segmented DMs [34][35], typically in combination with an array of single-mode optical fibers.

Monochromatic experiments in 2012 at the NASA/GSFC have yielded average contrasts of 5.1×10^{-9} at $2\lambda/D$ [36]. Separate experiments at JPL/Caltech have demonstrated the necessary wavefront sensing and control to phase the coronagraph. Coherent fiber bundles have been acquired and tested. The effort at NASA/GSFC is nearing the completion of its first milestone.

Work at NASA/GSFC has been led by Mark Clampin through a 2009 TDEM award; a technology milestone whitepaper was approved by the Program to formalize the goals of this research [38], whose results were under review in late 2012. Future efforts funded through 2010 SAT-TDEM awards will include the development of an engineering-model visible nuller by Richard Lyon (NASA/GSFC) and broadband contrast demonstrations by Jagmit Sandhu (JPL/Caltech) using the APEP facility.

Wavefront Sensing & Control

Self-Coherent Sensing

Coronagraphs may require integration times that are many hours long, not only to detect planets but also to sense wavefront errors. Coherent speckle detection methods may provide the means to more rapidly sense and correct wavefront errors. An approach similar to the Self-Coherent Camera [47] has been demonstrated in the HCIT using a pupil-plane mask with selectable pinholes. The goal was to demonstrate the capability to measure speckles of about 1×10^{-8} contrast with uncertainty, stability, and repeatability of 20% in intensity and 1 radian in phase with 90% statistical confidence, in a window at least 2×2 λ/D wide at $< 10\lambda/D$ from the star, in one spectral band of width ≥10%, with a uniform incoherent background of at least 1×10^{-8} in the area covered by the point-spread function [48]. This represents a related activity that may improve the stability of starlight-suppression experiments.

This work was conducted by Stuart Shaklan for Steven Kendrick (Ball Aerospace and Technology Corporation) and collaborators, funded through a 2009 TDEM award and successfully completed in 2012 [49].

Deformable Mirror Technology

As illustrated in Fig. A.1, wavefront aberrations less than 1/10,000th of a wave must be maintained if contrasts of 1×10^{-10} contrast are to be achieved in a coronagraph. At visible wavelengths, this implies wavefront control at the level of 0.5 Å, and deformable mirror (DM) technology is therefore required to compensate for residual optical aberrations. The state of the art in DM technology is represented by the Xinetics PMN mirrors, which are used routinely in the HCIT vacuum testbeds and have produced almost all the reported results of Fig. 2 (except those of the Visible Nulling Coronagraph), and all results with contrasts better than 1×10^{-9}.

The Xinetics PMN-based DMs have additionally been successfully vibration tested at JPL. Boston Micromachines MEMs DMs have undergone environmental testing [50] and have flown on a sounding rocket experiment [51], although in the latter case no performance data was acquired.

Through two separate 2010 TDEM awards, both Iris AO and Boston Micromachines Corp. have been funded to continue environmental testing of both continuous face-sheet DMs as well as segmented DMs, with the goal of better characterizing their failure modes, and thus raising the TRL of the respective DM models. Work to date has focused on establishing the testing protocols upon which the success criteria of the Whitepapers will be based. Paul Bierden is leading the effort on behalf of Boston Micromachines Corp. Michael Helmbrecht is leading the effort on behalf of Iris AO.

Modeling and Model Validation

Efficient Coronagraph Optical Modeling

New efficient implementations of coronagraph modelling for the Vector Vortex Coronagraph (VVC), the Phase-Induced Amplitude Apodization (PIAA) coronagraph, and the Hybrid Band-Limited Coronagraph (HBLC) have been shown to be accurate to 1% or better relative to the mean field contrast for contrasts down to 10^{-10} [44] [45]. This represents a related activity because it does not include experimental validation of the models, as required in Coronagraph Milestone 3A. Models developed through this work were used to predict coronagraph performance with realistic wavefront errors [46].

This work was the subject of a 2009 TDEM award to John Krist (JPL/Caltech) and collaborators. The effort was successfully completed and two technology milestone reports were approved by the Program [44] [46].

Model Validation of Band-limited Coronagraphs

To date no model of coronagraph performance has been experimentally validated, in the formal sense defined by TPF-C Milestone 3A. In 2011 initial work commenced to validate sensitivity models of band-limited coronagraphs using the same metallic mask used for TPF-C Milestone 2 [42]. Further progress was reported in 2012 [43].

The effort is being continued, led by Stuart Shaklan (JPL/Caltech) and funded through a 2010 SAT-TDEM award. The TPF-C Milestone 3A Whitepaper, provides the foundation for this work [18].

A.5 Starshade Milestones

External occulters, or starshades, block starlight by shadowing the entrance pupil of a telescope, using a physical separation between starshade and telescope sufficient to provide the necessary inner working angle. For a 4-m telescope this typically requires the starshade to be tens of meters in diameter and located tens of thousands of km from the telescope [52].

A starshade may have numerous petals that are each tapered to produce a desired apodization function, as seen from the telescope. The petal shapes also eliminate most edges that would otherwise diffract starlight toward the center of the image—thus suppressing the Poisson spot that would be present if a circular occulter were used. Independent optical modeling predictions have shown excellent agreement concerning the contrast sensitivity to petal shape errors [53], and detailed preliminary error budgets have been proposed [54].

There are two similar approaches to the design of external occulters currently being studied, differing by whether an analytical petal shape is used [55][56] or whether it derives from a mathematical optimization [57][58]. Two different implementations are being studied for the packaging and deployment of a starshade: the first would use deployable booms [59][60], while the second would use an unfurling truss [61][62].

The technology development for starshades may follow several parallel paths during pre-formulation. Unlike the case for the coronagraph, whose laboratory work unites many separate technologies in a progressive series of starlight suppression milestones, there are no comparable unifying milestones for the occulter. Because of the scale of the full space observatory, it is impossible to run full-scale tests of starlight suppression with such a system on the ground. Laboratory tests with subscale masks have yielded very encouraging results, but they do not demonstrate the key technology, described below, that would be needed for a space mission, nor validate error budgets that would be traceable to flight. The critical component and subsystem technologies can nonetheless be successfully demonstrated in pre-formulation, if pursued as separate parallel tasks. Therefore by the end of pre-formulation, modeling at the component, and subsystem level should enable the prediction of the future flight performance.

The subject areas for starshade milestones are listed below. In this list, the first Milestone topics are related to the materials, design, fabrication, and predicted optical performance of the as-built components and subsystems. The remaining milestones cover topics that must be demonstrated at the system level and include deployment, dynamic behavior, as well as guidance, navigation, and control. The final item is analogous to the final pre-formulation milestone for coronagraphs: a demonstration that the on-orbit performance is achievable based upon a well-grounded understanding of the error budget, backed by the necessary laboratory results.

- Petal manufacturing: Demonstrate that a single petal can be manufactured to the design tolerances. This may include a demonstration of the manufacturing of petal edges, tips, and valleys. A representative set of manufacturing tolerances shall be demonstrated that derive from error budget allocations.

- Control of scattered light: Demonstrate with a baseline external occulter design that the brightness of sunlight scattered from the occulter would be less than the brightness of exozodiacal light. This may include demonstrations of the control of light scattered from petal edges, transmitted through the occulter fabric, or reflected from other identified sources such as the Earth or Moon.

- Sub-component model validation: Demonstrate that the structural behavior of elements of a starshade can be predicted to the accuracy required for a flight mission. In the event that a test article is of a different size or configuration than the anticipated flight design, scaling laws will also be validated. This may include predictions of thermo-mechanical behavior based on known materials and structural properties as a function of temperature, anchored by coupon tests.

- Starshade deployment. Demonstrate that an external occulter can be deployed repeatedly to within the budgeted tolerances. This may be accomplished using single or multiple petals whose manufacturing tolerances have been demonstrated previously.

- Dynamic stability: Demonstrate that a deployed shape can be controlled to within the budgeted tolerances for anticipated flight conditions of science operations. This may include demonstrations of thermal and mechanical stability.

- Formation flying: Demonstrate that the guidance, navigation and control algorithms of an external occulter can achieve the budgeted alignment tolerances. This may include hardware and/or software simulations that demonstrate traceability to flight conditions.

- System modeling: Demonstrate through modeling, using subcomponent models and scaling laws that have been experimentally validated, combined with appropriate telescope models and the current mission error budget, that a full-size external occulter system could achieve a baseline contrast of 1×10^{-10} over the required optical bandwidth necessary for detecting Earth-like planets, characterizing their properties and assessing habitability.

By the end of Pre-Phase A, a sufficient number of demonstrations need to be made to establish with a high degree of confidence that a flight mission would be successful, based on a specific set of starshade technologies. Because there are two different technology paths being proposed for starshade packaging and deployment, the starshade structure and subcomponents may be very different in each approach. It follows that milestones accomplished for one approach might not be relevant to the technology advancement of the other.

A.5.1 Progress and Plans

Starlight Suppression Experiments

At Princeton University, the theoretical diffraction integral commonly used for occulter design has been optically validated for contrasts to 4.5×10^{-10} [63]. At Northrop Grumman Aerospace Systems (NGAS) starlight suppression experiments using scaled starshades have produced rotationally-averaged contrasts of 2.6×10^{-7} at the starshade mask's inner working angle—where the optical throughput drops to 50% [64]. Beyond the inner working angle yet within the apodized field-of-view, features as faint as 5×10^{-10} have also been detected through experiments both at Princeton University and at the University of Colorado.

These experiments are designed to measure the starshade's shadow at the same Fresnel number as would be used in an actual flight-system, although not with the same inner working angle. The masks are centimeters in diameter and placed at about ten or tens of meters from the detector. Research is ongoing at Princeton University in 2012-2013.

Precision Petal Manufacturing

An initial challenge of constructing a starshade is to demonstrate that the mechanical tolerances for a petal can be met, as derived from a complete starshade error budget. Prior work at NGAS demonstrated that precision petal tips and valleys are manufacturable to the required tolerances [65]. Work underway at Princeton University in 2012 has been directed toward the demonstration of a continuous petal edge, with a Milestone phrased as follows:

On a single full-scale petal made of flight-like materials, measure the edge position relative to a fiducial origin at a sufficient number of locations along the edge. Using optical modeling tools, verify that the predicted mean contrast in the image plane from a uniform field propagated past an occulter with petals of the measured shape in an annulus of width equal to the full-width half-max of the telescope point spread function at the smallest inner working angle is 3×10^{-10} or better, the allocated contrast to static errors. Repeat the measurements and analysis a sufficient number of times to give 95% confidence that the predicted contrast is correct [66] [67].

This work was conducted by N. J. Kasdin (Princeton University) and collaborators through a 2009 TDEM award and successfully completed in 2012 [67].

Starshade Petal Deployment

After the static mechanical tolerances are demonstrated, a subsequent challenge is to demonstrate that the deployment tolerances for a petal can be met, as derived from a complete starshade error budget. The concerns to be addressed here include not only the repeatability of deployment to within tolerances, but aspects of dynamic stability due to slow thermal changes, as might be experienced in flight.

Work will be conducted by N. J. Kasdin (Princeton University) and collaborators through a 2010 SAT-TDEM award. The goals of this effort have not yet been formalized by the Program.

A.6 Mid-Infrared Interferometry Milestones

Interferometry technology will ultimately provide higher angular resolution and thus the ability to detect and characterize a larger sample of exoplanets than is possible with either coronagraph or external occulter architectures. Interferometry at mid-infrared wavelengths has been pursued, because at these wavelengths there are good biosignatures for spectroscopy and the planet/star contrast is the highest. A summary of mid-infared interferometer milestones is given below, as described in the TPF-I Technology Plan [6]. Milestone 1 is a demonstration of adaptive correction of wavefront errors necessary to attain deep null depths. Milestone 3 is a demonstration of starlight suppression over a broad bandwidth using a two-element interferometer. Milestone 4 is a system demonstration using a four-element interferometer. Milestone 5 demonstrates the techniques of spectral fitting, which is the final step in starlight suppression necessary to detect exoplanets at mid-infrared wavelengths. These starlight suppression milestones are equally applicable to connected-structure and formation-flying concepts. Milestone 2 is a laboratory demonstration of formation-flying guidance, navigation & control.

Milestone 1. Using the Adaptive Nuller, demonstrate that optical beam amplitude can be controlled with a precision of ≤ 0.2% rms and phase with a precision of ≤ 5 nm rms over a spectral bandwidth of > 3 μm in the mid IR for two polarizations. This demonstrates the approach for compensating for optical imperfections that create instrument noise that can mask planet signals. This goal is consistent with starlight suppression of 1×10^5.

Milestone 2. Using the Formation Control Testbed (FCT) as an end-to-end system-level hardware testbed, demonstrate that a formation of multiple robots can autonomously initialize, maneuver and operate in a collision free manner. A key maneuver, representative of TPF-I science will be demonstrated by rotating through greater than 90° at ten times the flight rotation rate while maintaining a relative position control to 5 cm 1σ per axis. This is the first step in a full validation of the formation control architecture and algorithms and the testbed models developed by the Formation Algorithms & Simulation Testbed while physically demonstrating a scaled version of the approach to achieving the angular resolution required for the detection of terrestrial planets.

Milestone 3. Using either the Adaptive Nuller or the Achromatic Nulling Testbed, demonstrate that mid-infrared light in the 7–12 μm range can be suppressed by a factor of ≥ 10^5 over a waveband of ≥ 25%. This demonstrates the approach to broadband starlight suppression (dimming of light across a range of wavelengths) needed to characterize terrestrial planets for habitability. Flight-like nulls are to be demonstrated at room (non-flight) temperature.

Milestone 4. Using the Planet Detection Testbed, demonstrate detection of a simulated planet signal at a star/planet contrast ratio of $\geq 10^6$. This demonstrates that several opto-mechanical control loops can be integrated and operated in a testbed configuration that includes the principal functional blocks of the flight instrument. These functional blocks include fringe tracking, pathlength metrology, beam shear and pointing control, 4-beam combination and phase chopping. Success shows that an instrument can be operated with a stability representative of flight requirements and within about an order of magnitude of the contrast that permits the detection of the signal from an earth-like exoplanet in the habitable zone around a nearby star.

Milestone 5. Using the Planet Detection Testbed, demonstrate the starlight suppression technique of spectral fitting. The spectral fitting technique uses measurements that can be obtained from a broad band of nulled wavelengths to detect and remove the effect of opto-mechanical disturbances on the null, thereby effectively suppressing the starlight by another factor of ten.

A.6.1 Progress and Plans

Milestones 1, 2, 3, and 4 were completed by the TPF-I Pre-Project.

Laboratory demonstrations of interferometric nulling at mid-infrared wavelengths have been successful at reaching the performance needed to support a flight mission. The Milestone 1 demonstration of phase and intensity control of fringes was demonstrated at the required level [68]. The Milestone 3 demonstration of starlight suppression of 1×10^{-5}, was demonstrated with a 30% bandwidth [69] at such a level that the planet signal would be dominated by exozodiacal light, not starlight. The Milestone 4 system demonstration using two pairs of interferometers achieved contrasts of 1.65×10^{-8} in the lab using laser sources, with an experimental subtraction of noise using infrared chopping and averaging [70][71].

Work in progress on Milestone 5 is described below. In addition, further work is needed to demonstrate the same noise subtraction techniques over broader bandwidths and in a cryogenic environment. This would necessitate the testing of cryogenic mid-IR single-mode fibers, deformable mirrors, adaptive nullers, and more comprehensive system testing at liquid nitrogen temperatures.

Whereas a coronagraph architecture would be an extrapolation of existing space telescopes designs, it is very likely that an interferometer would have no precursor in space—whether it be a connected-structure design or a formation-flying mission. The Milestone 2 demonstrations of formation flying were successfully completed in a lab environment with hardware in the loop and 5-degrees of freedom for the two controlled satellites [72][73]. Nonetheless, the technology development for a formation flying interferometer may follow a path that includes one or more technology space missions prior to its full implementation.

In 2011 the Planet Detection Testbed was modified and upgraded to include a broadband mid-infrared detector for use with Milestone 5. This milestone would complete the suite of room-temperature starlight suppression experiments that had been planned for mid-infrared interferometry. A formal Milestone Whitepaper was approved by the Program [74], milestone experiments were attempted, but this effort was halted for funding reasons in September 2011.

A.7 Other Milestones

Detector Technology*

Donald Figer (Rochester Institute of Technology) was funded through a 2009 SAT-TDEM award to raise the technology readiness of Avanlanche Photodiode (APD) arrays. A formal Milestone Whitepaper was approved by the Program for this effort [75]. The Milestone was phrased as follows:

Demonstrate the performance of a photon-counting 256×256 Geiger-Mode Avalanche Photodiode (GM-APD) focal plane array after radiation exposure. The array is designed to provide zero read-noise, ultra-high dynamic range, and highly linear response. The following characteristics are to be measured: dark current, intra-pixel response, total quantum efficiency, after-pulsing, persistent charge, and crosstalk. The measurements will be made before and after 50 krad (Si) ~60 MeV proton irradiation. Important performance parameters include read noise, dark counts, and total quantum efficiency. This work is being conducted through the Rochester Institute of Technology.

This effort is a demonstration of new detector technology that may greatly improve the science throughput of coronagraph and starshade mission concepts. This work is ongoing: a silicon 256×256 diode array has been bonded to a Read Out Integrated Circuit (ROIC); the array has been hybridized and tested [76]; and a first-light image has been obtained. This device has a 100% fill factor and a good response from 300–1000 nm. Preparations are now underway for radiation testing. Future work in this area may include the performance validation of silicon focal plane arrays with a larger number of pixels (1024×1024 vs 256×256).

* This topic was selected as part of the 2009 ROSES TDEM solicitation, but was excluded from subsequent ROSES solicitations.

A.8 Conclusion

The 2010 Astrophysics Decadal Survey recommended the creation of a technology development program for a potential future exoplanet mission to mature starlight-suppression technology for the detection of spectra of Earth-like exoplanets. The Exoplanet Exploration Program supports a community-based process to help NASA select a single architecture by about 2015, and to mature the selected concept for recommendation in the 2020 Decadal Survey. This appendix outlines technology development that will lead toward that goal.

A new appendix will be released each year to update the progress made in each technology area and to identify new SAT-TDEM selections.

A.9 Bibliography

[1] NRC Astronomy and Astrophysics Survey Committee, New Worlds, New Horizons in Astronomy and Astrophysics, The National Academies Press, Washington, DC, 2010.

[2] Traub, W. A., & Oppenheimer, B. R. 2010, "Direct Imaging of Exoplanets," in *Exoplanets*, Seager, S., ed., University of Arizona Press, pp. 111–156.

[3] Mawet, D., Pueyo, L., Lawson, P., et al. 2012, "Review of small-angle coronagraphic techniques in the wake of ground-based second-generation adaptive optics systems," Proc. SPIE 8442, 844204.

[4] Levine, M., Shaklan, S., & Kasting, J. 2005, eds., Terrestrial Planet Finder Coronagraph Science and Technology Definition Team (STDT) Report, Jet Propulsion Laboratory Publications, Pasadena, California, JPL Document 34923, June 2005.

[5] Lawson, P. R., Lay, O. P., Johnston, K. J., & Beichman, C. A., eds., The Terrestrial Planet Finder Interferometer Science Working Group Report, Jet Propulsion Laboratory, Pasadena, California, JPL Pub. 07-1, March 2007.

[6] Lawson, P. R., & Dooley, J. A., eds. 2005, Technology Plan for the Terrestrial Planet Finder Interferometer, Jet Propulsion Laboratory Publications, Pasadena, California, JPL Pub. 05-5, June 2005.

[7] Dooley, J. A., & Lawson, P. R., eds. 2005, Technology Plan for the Terrestrial Planet Finder Coronagraph, Jet Propulsion Laboratory Publications, Pasadena, California, JPL Pub. 05-8, March 2005.

[8] Trauger, J. T., & Traub, W. A. 2007, "A laboratory demonstration of the capability to image an Earth-like extrasolar planet," Nature 446, pp. 771–773.

[9] Mawet, D., Serabyn, E., Liewer, K., et al. 2009, "Optical Vectorial Vortex Coronagraphs using Liquid Crystal Polymers: theory, manufacturing and laboratory demonstration," Optics Express 17, pp. 1902–1918.

[10] Guyon, O. 2003, "Phase-induced amplitude apodization of telescope pupils for extrasolar terrestrial planet imaging," Astron. Astrophys. 404, pp. 379–387.

[11] Kasdin, N. J., Carlotti, A., Pueyo, L., Groff, T., Vanderbei, R. 2011, "Unified coronagraph and wavefront control design," Proc. SPIE 8151, 81510Y

[12] Lyon, R. G., Clampin, M., Woodruff, R. A., et al. 2010, "Visible nulling coronagraphy testbed development for exoplanet detection," Proc. SPIE 7731.

[13] Moody, D. C., Gordon, B. L., & Trauger, J. T. 2008, "Design and demonstration of hybrid Lyot coronagraph masks for improved spectral bandwidth and throughput," Proc. SPIE 7010.

[14] Trauger, J., Moody, D., Gordon, B., Krist, J., Mawet, D. 2011, "A hybrid Lyot Coronagraph for the direct imaging and spectroscopy of exoplanet systems," Proc. SPIE 8151, 81510G.

[15] Kern, B., Kuhnert, A., & Trauger, J. 2008, eds., Exoplanet Exploration Technology Milestone #2 Report, Jet Propulsion Laboratory Publications, Pasadena, California, JPL Document 60951.

[16] Trauger, J., Stapelfeldt, K., Traub, W., et al. 2010, "ACCESS: a concept study for the direct imaging and spectroscopy of exoplanetary systems," Proc. SPIE 7731, pp. 773128–+.

[17] Trauger, T., Kern, B., & Kuhnert A., eds., 2006, TPF-C Technology Milestone #1 Report, Jet Propulsion Laboratory Publications, Pasadena, California, JPL Document 35484.

[18] Shaklan, S., 2009, Exoplanet Exploration Coronagraph Technology Milestone #3A White Paper: Coronagraph Stalight Suppression Model Validation, Jet Propulsion Laboratory Publications, Pasadena, California, JPL Document 64582.

[19] Soummer, R., Pueyo, L., Ferrari, A., et al. 2009, "Apodized pupil Lyot coronagraphs for arbitrary apertures. II. Theoretical properties and application to extremely large telescopes," Astrophys. J. 695, 695-706.

[20] Mawet, D., Serabyn, E., Wallace, J. K., & Pueyo, L. 2011, "Improved high-contrast imaging with on-axis telescopes using a multistage vortex coronagraph," Opt. Lett. 36, 1506-1508.

[21] Guyon, O., Kern, B., Belikov, R., et al. 2012, "Phase Induced Amplitude Apodization (PIAA) coronagraphy: Recent results and future prospects," Proc. SPIE 8442, 84424V.

[22] Carlotti, A., Kasdin, N. J., Vanderbei, R. J., Delorme, J.-R. 2012, "Optimized shaped pupil masks for pupil with obscuration," Proc. SPIE 8442, 844254.

[23] Trauger, J., Gordon, B., Krist, J. et al. 2010, "Technology Milestone Whitepaper: Hybrid Lyot Coronagraph Technology – Linear Masks," Jet Propulsion Laboratory Doc. D-64843. http://exep.jpl.nasa.gov/technology.

[24] Trauger, J., Moody, D., Gordon, B., Krist, J., and Mawet, D. 2012, "Complex apodization Lyot coronagraphy for the direct imaging of exoplanet systems: design, fabrication, and laboratory demonstration," Proc. SPIE 8442, 84424Q.

[25] Belikov, R., Pluzhnik, Witteborn, F. C., et al. 2011, "Laboratory demonstration of high-contrast imaging at inner working angles better than 2 λ/D and better," Proc. SPIE 8151, 815102.

[26] Kern, B., Guyon, O., Give'on, A., Kuhnert, A., Niessner, A. 2011, "Laboratory testing of a Phase-Induced Amplitude Apodization (PIAA) coronagraph," Proc. SPIE 8151, 815104.

[27] Guyon, O., Schneider, G., Close, L. et al. 2010, "Technology Milestone Whitepaper: Phase-Induced Amplitude Apodization Coronagraph: Monochromatic Contrast Demonstration," Jet Propulsion Laboratory Doc. D-65830. http://exep.jpl.nasa.gov/technology.

[28] Guyon, O., Schneider, G., Close, L., et al. 2011, "Technology Milestone #2 Whitepaper: Instrument Tip-Tilt Control Demonstration at the sub-Milliarcsecond Level," Jet Propulsion Laboratory Doc. D-71066. http://exep.jpl.nasa.gov/technology.

[29] Guyon, O., Kern, B., Belikov, R., et al. 2012, "Phase Induced Amplitude Apodization (PIAA) coronagraphy: Recent results and future prospects," Proc. SPIE 8442, 84424V.

[30] Mawet, D. P., Serabyn, E., Moody, D., et al. 2011, "Recent results of the second generation of vector vortex coronagraphs on the High Contrast Imaging Testbed at JPL," Proc. SPIE 8151, 81511D.

[31] Serabyn, E., Mawet, D., Burruss, R. 2010, "An image of an exoplanet separated by two diffraction beamwidths from a star," Nature 464, 1018.

[32] Mawet, D., Serabyn, E., Wallace, J. K., et al. 2011, "Improved high-contrast imaging with on-axis telescopes using a multistage vortex coronagraph," Opt. Lett. 36, 1506.

[33] Serabyn, G., Krist, J., Mawet, D., Moody, D., and Trauger, J. 2012, "Technology Milestone Whitepaper: Vortex Coronagraph Technology," Jet Propulsion Laboratory Doc. D-73329. http://exep.jpl.nasa.gov/technology.

[34] Stewart, J. B., Bifano, T. G., Cornelissen, S., Bierden, P., Levine, B. M., Cook, T. 2007, "Design and development of a 331-segment tip-tilt-piston mirror array for space-based adaptive optics," Sensors and Actuators A 138, 230-238.

[35] Helmbrecht, M. A., He, M., Kempf, C. J. 2012, "Development of high-order segmented MEMS deformable mirrors," Proc. SPIE 8253, 825307.

[36] Lyon, R. G., Clampin, M., Petrone, P., Mallik, U., Madison, T., and Bolcar, M. R. 2012, "High contrast Vacuum Nuller Testbed (VNT) contrast, performance and null control," Proc. SPIE 8442, 844208.

[37] Lyon, R. G., Clampin, M., Petrone, P., et al. 2011, "Vacuum nuller testbed (VNT) performance, characterization and null control: progress report," Proc. SPIE 8151, 81510G.

[38] Clampin, M. 2011, "Technology Milestone #1 Whitepaper: Visible Nulling Coronagraph Technology Maturation: High Contrast Imaging and Characterization of Exoplanets," Jet Propulsion Laboratory Doc. D-68671. http://exep.jpl.nasa.gov/technology.

[39] Belikov, R., Give'on, A., Kern, B., et al. 2007, "Demonstration of high contrast in 10% broadband light with the shaped pupil coronagraph," Proc. SPIE 6693.

[40] Pueyo, L., Kay, J., Kasdin, N. J., et al. 2009, "Optimal dark hole generation via two deformable mirrors with stroke minimization," Appl. Opt. 48, pp. 6296–6312.

[41] Groff, T. D., Kasdin, N. J., Carlotti, A., and Eldorado Riggs, A. J. 2012, "Broadband focal plane wavefront control of amplitude and phase aberrations," Proc. SPIE 8442, 84420C.

[42] Sidick, E., Shaklan, S., Give'on, A., Kern, B. 2011, "Studies of the effects of optical system errors on the HCIT contrast performance," Proc. SPIE 8151, 815106.

[43] Sidick, E., Shaklan, S., Balasubramanian, K. 2012, "HCIT broadband contrast performance sensitivity studies," Proc. SPIE 8520, 85200M.

[44] Krist, J., Belikov, R., Mawet D. et al. 2012, "Technology Milestone #1 Report: Assessing the performance limits of internal coronagraphs through end-to-end modelling," Jet Propulsion Laboratory Doc. D-74425. http://exep.jpl.nasa.gov/technology.

[45] Krist, J. E., Belikov, R., Pueyo, L., et al. 2011, "Assessing the performance limits of internal coronagraphs through end-to-end modelling: a NASA TDEM study," Proc. SPIE 8151, 81510E.

[46] Krist, J., Belikov, R., Mawet D. et al. 2012, "Technology Milestone #2 Report: Assessing the performance limits of internal coronagraphs through end-to-end modelling," Jet Propulsion Laboratory Doc. D-74426. http://exep.jpl.nasa.gov/technology.

[47] Galicher, R., Baudoz, P., Rousset, G., et al. 2010, "Self-coherent camera as a focal plane wavefront sensor: simulations," A&A 509, A.31.

[48] Give'on, A., Shaklan, S., Kern, B., Noecker, C., Kendrick, S., and Wallace, K. 2012, "Electric field reconstruction in the image plane of a high-contrast coronagraph using a set of pinholes around the Lyot plane," Proc. SPIE 8442, 84420B.

[49] Shaklan, S., Kern, B., Give'on, A., et al. 2012, "Technology Milestone Report: Advancing Speckle Sensing for Internal Coronagraphs," Jet Propulsion Laboratory Document D-73509. http://exep.jpl.nasa.gov/technology.

[50] Enya, K., Abe, L., Takeuchi, S., et al., 2011, "A high dynamic-range instrument for SPICA for coronagraphic observation of exoplanets and monitoring of transiting exoplanets," Proc. SPIE 8146, 81460Q.

[51] Mendillo, C. B., Hicks, B. A., Cook, T. A., et al. 2012, "PICTURE: a sounding rocket experiment for direct imaging of an extrasolar planetary environment," Proc. SPIE 8442, 84420E.

[52] Turnbull, M. C., Glassman, T., Roberge, A., et al. 2012, "The search for habitable worlds. 1: The viability of a starshade mission," Pub. Astron. Soc. Pac. 124, 418-447.

[53] Shaklan, S. B., Noecker, M. C., Glassman, T., et al. 2010, "Error budgeting and tolerancing of starshades for exoplanet detection," Proc. SPIE 7731, 77312G.

[54] Shaklan, S. B., Marchen, L., Lisman, P. D., et al. 2011, "A starshade petal error budget for exo-earth detection and characterization," Proc. SPIE 8151, 815113.

[55] Copi, C. J., and Starkman, G. D. 2000, "The Big Occulting Steerable Satellite (BOSS)," Astrophys. J. 532, 581–592.

[56] Cash, W. 2006, "Detection of Earth-like planets around nearby stars using a petal-shaped occulter," Nature 442, pp. 51–53.

[57] Vanderbei, R. J., Cady, E., & Kasdin, N. J. 2007, "Optimal Occulter Design for Finding Extrasolar Planets," Astrophys. J. 665, pp. 794–798.

[58] Cady, E. 2011, "Nondimensional representations for occulter design and performance evaluation," Proc. SPIE 8151, 815112.

[59] Lo, A., Cash, W., Hyde, T., Polidan, R., & Glassman, T. 2009, "Starshade Technology Development: Astro2010 Technology Development Whitepaper," ArXiv Astrophysics e-prints 2010, pp. 44–+.

[60] Cash, W., Kendrick, S., Noecker, et al., 2009, "The New Worlds Observer: the astrophysics strategic mission concept study," Proc. SPIE 7436.

[61] Thomson, M. W., Lisman, P. D., Helms, R., et al. 2010, "Starshade design for occulter based exoplanet missions," SPIE 7731.

[62] Kasdin, N. J., Spergel, D. N., Lisman, D., et al. 2011, "Advancing technology for starlight suppression via an external occulter," Proc. SPIE 8151, 81510J.

[63] Sirbu, D., Cady, E., Kasdin, N. J., et al. 2011, "Optical verification of occulter-based high contrast imaging," Proc. SPIE 8151, 815114.

[64] Samuele, R., Varshneya, R., Johnson, T. P., et al. 2010, "Progress at the starshade testbed at Northrop Grumman Aerospace Systems: comparisons with computer simulations," Proc. SPIE 7731.

[65] Lo, A. S., Glassman, T., Dailey, D., Sterk, K., Green, J., Cash, W., Soummer, R. 2010, "New Worlds Probe," Proc. SPIE 7731, 77312E.

[66] Kasdin, N. J., Lisman, D., Shaklan, S., et al. 2012, "Technology demonstration of starshade manufacturing for NASA's Exoplanet Mission Program," Proc. SPIE 8442, 84420A.

[67] Kasdin, N. J., Spergel, D. N., Vaderbei, R., et al. 2012, "Technology Milestone Report: Advancing Technology for Starlight Suppression via an External Occulter," Jet Propulsion Laboratory Document D-74384. http://exep.jpl.nasa.gov/technology.

[68] Peters, R. D., Lay, O. P., & Jeganathan, M. 2008, "Broadband phase and intensity compensation with a deformable mirror for an interferometric nuller," Appl. Opt. 47, pp. 3920–3926.

[69] Peters, R. D., Lay, O. P., & Lawson, P. R. 2010, "Mid-infrared adaptive nulling for the detection of Earth-like exoplanets," Pub. Astron. Soc. Pac. 122, pp. 85–92.

[70] Martin, S. R., & Booth, A. J. 2010, "Demonstration of exoplanet detection using an infrared telescope array," Astron. Astrophys. 520, pp. A96+.

[71] Martin, S. R., & Booth, A. J. 2010, "Strong starlight suppression sufficient to enable direct detection of exoplanets in the habitable zone," Astron. Astrophys. 511, pp. L1+.

[72] Scharf, D. P., Keim, J. A., and Hadaegh, F. Y. 2010, "Flight-like ground demonstrations of precision maneuvers for spacecraft formations: Part I," IEEE Systems J. 4, pp. 84–95.

[73] Scharf, D. P., Keim, J. A., and Hadaegh, F. Y. 2010, "Flight-like ground demonstrations of precision maneuvers for spacecraft formations: Part II," IEEE Systems J. 4, pp. 96–106.

[74] Martin, S. R., and Lay, O. P. 2010, "Exoplanet Interferometry Technology Milestone #5 Whitepaper: Spectral Fitting and Planet Detection Demonstration," Jet Propulsion Laboratory Doc. D-66389. http://exep.jpl.nasa.gov/technology.

[75] Figer, D. 2010, "Technology Milestone Whitepaper: A Photon-Counting Detector for Exoplanet Missions," Jet Propulsion Laboratory Doc. D-66493. http://exep.jpl.nasa.gov/technology.

[76] Figer, D., Lee, J., Hanold, B. J., et al. 2011, "A photon-counting detector for exoplanet missions," Proc. SPIE 8151, 81510K.